Chemical Science

ROYAL SOCIETY OF CHEMISTRY

EDGE ARTICLE

View Article Online
View Journal | View Issue

Cite this: *Chem. Sci.*, 2024, **15**, 12098

All publication charges for this article have been paid for by the Royal Society of Chemistry

Received 16th April 2024
Accepted 26th June 2024

DOI: 10.1039/d4sc02514h

rsc.li/chemical-science

Real-time observation of sub-100-fs charge and energy transfer processes in DNA dinucleotides†

Vasilis Petropoulos, [a] Lara Martinez-Fernandez,*[b] Lorenzo Uboldi, [a] Margherita Maiuri, [a] Giulio Cerullo, *[ac] Evangelos Balanikas [d] and Dimitra Markovitsi *[e]

Using as showcase the DNA dinucleotide 5′-dTpdG-3′, in which the thymine (T) is located at the 5′ end with respect to the guanine (G), we study the photoinduced electronic relaxation of coupled chromophores in solution with an unprecedented refinement. On the one hand, transient absorption spectra are recorded from 20 fs to 45 ps over the 330–650 nm range with a temporal resolution of 30 fs; on the other hand, quantum chemistry calculations determine the ground state geometry of the 4 possible conformers with stacked nucleobases, the associated Franck–Condon states, and map the relaxation pathways leading to excited state minima. Important spectral changes occurring before 100 fs are correlated with concomitant $G^+ \rightarrow T^-$ charge transfer and T → G energy transfer processes. The lifetime of the excited charge transfer state is only 5 ps and the absorption spectrum of a long-lived $n\pi^*T$ state is detected. Our experimental results match the transient spectral properties computed for the *anti–syn* conformer of 5′-dTpdG-3′, which is characterized by the lowest ground state energy and differs from that encountered in B-form duplexes.

Introduction

Excited state relaxation in DNA is studied in relation with its damage induced by absorption of UV radiation[1] and in view of future developments of DNA-based label-free optoelectronic devices.[2,3] In both cases, charge and energy transfer processes play a key role. For example, the formation of the carcinogenic (6–4) photo-adducts,[4] as well as charge carrier generation by low-energy photons,[5] involve the population of an excited charge transfer (*CT*) state,[6] in which an atomic charge has been transferred between two stacked nucleobases. Similarly, excitation energy transfer (*ET*) among nucleobases has been shown to provoke remote photodamage.[7]

Numerous transient absorption (*TA*) studies have characterized the decay of *CT* states in various types of DNA multimers, ranging from dinucleotides and single strands to duplexes and guanine quadruplexes (G-Quadruplexes).[8–22] However, the formation of these states from the excited states initially populated upon photon absorption (Franck–Condon states) has not been observed in real time. Likewise, *ET* was inferred from the fluorescence anisotropy values detected once the process has occurred.[23] The main reason for the lack of direct experimental observation is that these processes are faster than the time resolution of the ultrafast spectroscopy setups used to date in these studies, which is typically in the 150–300 fs range.

A second, albeit equally important, difficulty is conceptual. So far, the data derived from *TA* experiments have been analysed using multiexponential functions, and time constants were correlated with monomer excited states and *CT* states (often referred as exciplexes/excimers). However, this approach becomes problematic when wave packets evolve along potential energy surfaces (*PES*). The latter do not fulfil the requirements for exponential decays, which are valid when the interactions of the chromophore with its environment are uniform in the three-dimensional space. They fall instead in the category of restricted geometries, in which dynamics has been discussed for a large variety of processes and systems.[24–29]

Here, we report the first comprehensive study monitoring the progression of electronic excitations from the Franck–Condon states to the *PES* minima in DNA multimers. We use as a showcase the DNA dinucleotide 5′-dTpdG-3′, abbreviated as **TG**, in which the thymine (T) is located at the 5′ end and the guanine (G) at the 3′ end. The investigation of dinucleotides by

[a]*Dipartimento di Fisica, Politecnico di Milano, Piazza Leonardo da Vinci 32, I-20133 Milano, Italy. E-mail: giulio.cerullo@polimi.it*

[b]*Instituto de Química Física Blas Cabrera, Consejo Superior de Investigaciones Científicas, Calle Serrano 119, Madrid, 28006, Spain. E-mail: lmartinez@iqf.csic.es*

[c]*Istituto di Fotonica e Nanotecnologie-CNR, Piazza Leonardo da Vinci 32, I-20133 Milano, Italy*

[d]*Department of Physical Chemistry, University of Geneva, CH-1211 Geneva-4, Switzerland*

[e]*Université Paris-Saclay, CNRS, Institut de Chimie Physique, UMR8000, 91405 Orsay, France. E-mail: dimitra.markovitsi@universite-paris-saclay.fr*

† Electronic supplementary information (ESI) available. See DOI: https://doi.org/10.1039/d4sc02514h

TA[8–14] spectroscopy has proved helpful in disentangling processes in larger systems, in which a multitude of interactions are operative. In addition to being a convenient model system, the 5′-dTpdG-3′ sequence is frequently encountered in G-Quadruplexes. Thymines located at the 5′ position with respect to the G-core have important implications on the geometry adopted by these four-stranded structures.[30]

Our *TA* experiments are performed with an unprecedented combination of temporal resolution and spectral coverage;[31] *TA* spectra (*TAS*) following resonant photoexcitation by ≈25 fs pulses at 266 nm are recorded from 20 fs to 45 ps over the 330–650 nm range with a temporal resolution of ≈30 fs, as discussed in Section 1 of the ESI.† In parallel, quantum chemistry calculations determine the associated Franck–Condon excited states of the four possible conformers with stacked nucleobases, and map the relaxation pathways leading to excited state minima for all of them. The *TAS* corresponding to the most stable conformer are also computed. We show that the evolution from the Franck–Condon states toward these minima is manifested by an ultrafast spectral shift occurring with half-time ($\tau_{1/2}$) of 50 fs. Moreover, along with the formation of the $G^+ \rightarrow T^-$ *CT* state, we detect an ultrafast T → G *ET*. In a more general way, this is the first comprehensive study of photoinduced processes on bichromophoric systems performed with such refinement, *i.e.* detecting several transient species over a broad spectral range at early times and identifying them *via* the shapes of their *TAS*.

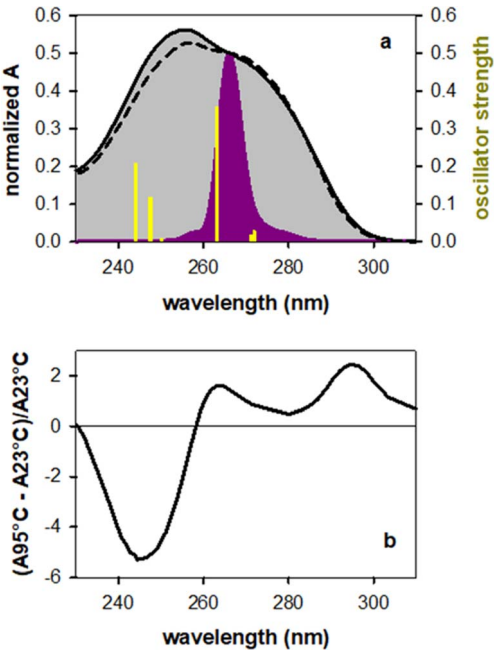

Fig. 1 (a) Steady-state absorption spectra recorded for **TG** (solid lines) and an equimolar mixture of dT and dG (dashed lines) normalized at the peak wavelength (266 nm) of the exciting laser pulse (violet); yellow sticks correspond to the electronic transitions computed for the *anti–syn* **TG** conformer. (b) Difference between the steady-state absorption spectra recorded for **TG** at 95° ($A_{95\ °C}$) and at 23 °C ($A_{23\ °C}$), divided by ($A_{23\ °C}$).

Results and discussion

Ground state properties

Fig. 1a shows the steady-state absorption spectrum of **TG** together with that of an equimolar mixture of the mononucleosides thymidine (dT) and deoxyguanosine (dG), their intensity being normalized at the peak wavelength of the laser pulse (266 nm). At this wavelength the molar absorption coefficients of dT and dG are the same.[32] The maximum of the **TG** spectrum is slightly blue-shifted with respect to that of monomers (254 *vs.* 257 nm) and its intensity is somewhat higher, suggesting chromophore coupling. Base stacking in DNA is commonly detected by changes in the molar absorption coefficient upon heating (hypochromism/hyperchromism). This temperature dependence is explained by the fact that orbital overlap among stacked nucleobases leads to coupling between ππ* and *CT* transitions.[33,34] Such changes are indeed observed in the difference of the absorption spectra recorded for **TG** at 95 °C and 23 °C (Fig. 1b), confirming base stacking. As reported in the literature,[9,14] these changes in dinucleotides do not exceed a few percent.

In order to determine the stacking patterns, we optimized the four possible stacking geometries, *anti–anti*, *anti–syn*, *syn–anti* and *syn–syn* (Fig. 2), where *anti* and *syn* refer to the position of each nucleobase (in the order T-G) with respect to the angle of the glycosidic bond (Fig. S2†), associated with the deoxyribose moiety.

The energy of the *anti–syn* conformer is lower, respectively, by 0.06, 0.19 and 0.17 eV than those of the three other conformers (Fig. 2 and Table S1†). These values are higher than the thermal energy at room temperature (0.025 eV), making *anti–syn* **TG** the most stable conformer. Therefore, we show detailed results for this conformer. However, in order to get a global picture, we also compute the Franck–Condon excited states and the associated relaxation pathways for the *syn–anti* and *syn–syn* conformers, and refine those of the *anti–anti* **TG**, whose properties were reported in ref. 35.

The properties of the 6 Franck–Condon states of *anti–syn* **TG** are shown in Table 1 and the difference in the electronic density between their ground and excited state in Fig. S3.† Among them, S_3, S_5 and S_6, having an oscillator strength higher than 0.1, are most likely to be populated by the exciting laser pulse. S_3 is a ππ*T state, encompassing a very weak (0.08 a.u.) $G^+ \rightarrow T^-$ *CT*. A larger *CT* (0.57 a.u.) characterizes the S_5 state, while S_6 results from a mixing of the ππ*G (La) state with weak *CT* (0.20 a.u.). The omnipresence of the *CT* is understandable, because G and dT are the nucleobases with the highest oxidation and the lowest reduction potential, respectively.[36] All 6 states are represented as sticks in Fig. 1a. We note that the energy of the S_5 state coincides with that of the ππ*(Lb) state in the free guanosine chromophore, which is readily excited at 267 nm.[32,37–39] Interestingly, no ππ*G(Lb) was identified for *anti–syn* **TG** in the examined spectral range.

The properties of the Franck–Condon states of the three other conformers are presented in Tables S2, S3 and S4.† By comparing these states determined for all four conformers, we remark that the *CT* character is favoured when at least one base

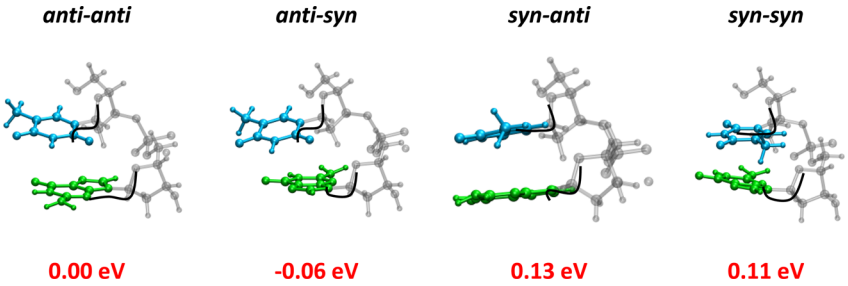

Fig. 2 Ground state structures of the four possible conformers with stacked nucleobases computed for **TG** and their relative energies (Δ*G*, in red). Thymine in blue; guanine in green. The dihedral angles that determine the *syn* and *anti* conformations are indicated in black.

Table 1 Properties of the Franck–Condon states determined for *anti–syn* **TG** at the PCM/M052X/6-31G(d) level of theory. VAE: vertical absorption energy; *f*: oscillator strength; *δ*: charge transfer character

State	Character	VAE (eV)	*f*	*δ* (a.u.)
S_1	nπ*(T) + ππ*G(La)	5.21	0.0295	0.01
S_2	ππ*G(La) + nπ*(T)	5.22	0.0192	0.02
S_3	ππ*T + G → T *CT*	5.36	0.3573	0.08
S_4	nπ*G(La)	5.61	0.0093	0.01
S_5	G → T *CT*	5.66	0.1188	0.57
S_6	ππ*G(La) + G → T *CT*	5.73	0.2099	0.20

presents *syn* orientation. Indeed, no state with significant (>0.3 a.u.) *CT* is encountered below the S_{10} for the *anti–anti* conformer, whereas for the *anti–syn* and *syn–syn* conformers the S_5/S_6 states are characterized by a *CT* contribution. This trend is more pronounced in the case of the *syn–anti* conformer, for which the lowest-lying bright ππ* states (S_2 and S_4) exhibit modest (0.3–0.4 a.u.) *CT* character.

Transient absorption spectra and dynamics

The experimental *TAS* recorded for **TG**, presented in Fig. 3, consist of a broad photoinduced absorption (*PA*) band whose shape and intensity evolve with time. Their comparison with the *TAS* of an equimolar mixture of dT and dG at selected times reveals important differences (Fig. 3a), further confirming the existence of significant electronic coupling between the nucleobases, in line with the steady-state spectra in Fig. 1. In particular, the negative signal, stemming from stimulated emission (*SE*) of the thymidine chromophore (Fig. S4†), already reported in the literature,[11,40] is completely absent from the *TAS* of the dinucleotide. Thus, it appears that the contribution of the ππ*T state, either correlated with unstacked nucleobases or present as a localized state within stacked ones, is significantly lower than what is expected for a solution containing 50% dT chromophores. However, we cannot rule out the presence of a weak *SE*, peaking below 400 nm, which may overlap with the UV *PA* band and decrease its intensity. Consequently, at early times, we focus mainly on the spectral changes in the visible spectral range.

Focusing on the evolution of the **TG** *TAS*, we observe that, at early times (Fig. 3b), their intensity increases with the time, while the maximum of the low-energy band moves from 602 to 565 nm. The dynamics of the shift can be approximated by a power law $\alpha t^{-0.04}$ (Fig. 4a), the $\tau_{1/2}$ being 50 fs. After 100 fs, the intensity in the visible starts decreasing slowly, while the shift toward shorter wavelengths persists, albeit at a significantly slower rate (Fig. 3c). In this case, the spectral shift can be described by a mono-exponential function with a time constant of 0.61 ± 0.08 ps (Fig. 4b). The maximum of the low-energy band is located at 530 nm at 3 ps. After this time, when the monomer signals have practically disappeared, the decay of the low-energy band is also described by a mono-exponential function with a time constant of 5.44 ± 0.03 ps (Fig. 4c). Following this decay, a long-lived background *PA* remains (Fig. 3a).

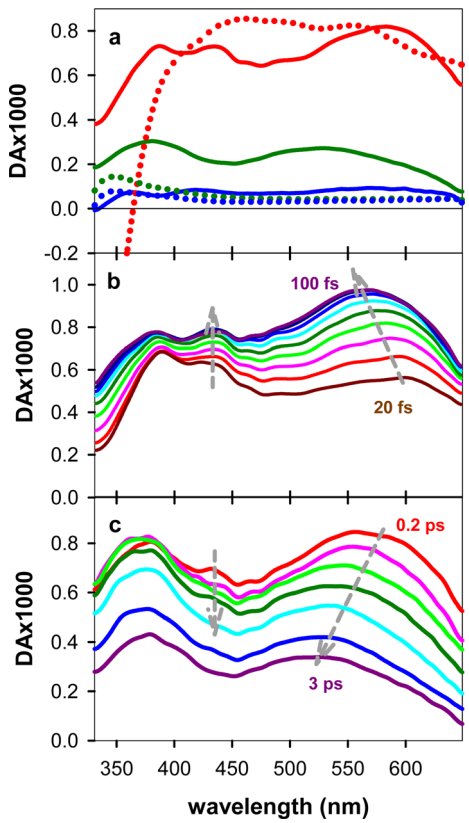

Fig. 3 *TAS* recorded for **TG** (solid lines) and an equimolar mixture of dT and dG (dots). (a) 50 fs (red), 5 ps (green) and 40 ps (blue). (b) From 20 to 100 fs with 10 fs steps. (c) 0.2 ps (red), 0.3 ps (pink), 0.4 ps (light green), 0.6 ps (dark green), 1 ps (cyan), 2 ps (blue) and 3 ps (violet).

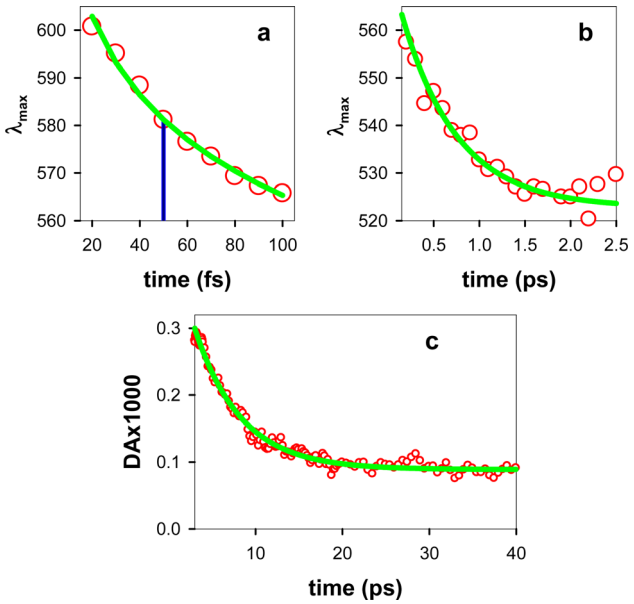

Fig. 4 Photo-induced dynamics (red circles) observed for **TG** over 3 timescales. (a) and (b) peak position (λ_{max}) of the low-energy band. (c) Decay of the *TA* signal at 570 nm. Green lines correspond to fits with a power law (a) and mono-exponential (b and c) functions. The blue line in (a) indicates $\tau_{1/2}$.

Computed relaxation paths

In order to get an insight into the origin of the above-described spectral evolution, we computationally mapped the deactivation pathways for the first 5 low-energy Franck–Condon states, plus the one exhibiting the largest charge transfer. For *anti–syn* **TG**, we identified three minima in the *PES* of the first excited states: min-ππ*G (La), min-*CT* and min-nπ*T (Table S5†). The pathway leading from S_3, which has predominantly ππ*T character, to min-ππ*G corresponds to a T → G *ET*. S_5 leads to min-*CT*, where an electric charge of 0.81 a.u. has been transferred from G to T. The min-nπ*T is reached following internal conversion from the S_2 and S_4 states, and, since the former state is not completely dark, we also expect weak population of this minimum.

The various relaxation pathways are schematically illustrated in Fig. 5; details are given in Table S5.† We stress that during the optimization procedure more than one reaction coordinate was varied. However, for two of the minima, one coordinate undergoes larger modifications than the others: the min-ππ*G strongly distorts the C_2–NH_2 coordinate whereas the min-nπ*T moves the O_4 out of the plane (atom labelling in Fig. S5†). In the case of the min-*CT* there is a global rearrangement of the inter-base distance and displacements, plus some modifications in the thymine aromatic ring.

Similar calculations were performed for the three other conformers. The results are summarized in Tables S6, S7 and S8.† For *anti–anti* **TG**, three minima, min-ππ*G (La), min-ππ*T and min-nπ*T, were also determined. In agreement with the higher stability of the *CT* states at the Franck–Condon region, mentioned above for the "*syn*" conformers, a min-*CT* was optimized for the *syn–anti* conformer, while for *syn–syn* **TG** a conical intersection between the first excited and the ground state exhibiting *CT* character was found.

The *TAS* computed for the Franck–Condon states of *anti–syn* **TG** with the highest oscillator strength (Tables 1, S_3, S_5 and S_6†) are presented in Fig. S6† together with the corresponding minima. We remark a clear trend: the spectra of the minima are all blue-shifted with respect to those of the initial states.

Assignment of the observed spectral evolution

Next, we search the fingerprints of the above-described relaxation pathways in the experimental *TAS*, starting from the long times. We also discuss these data in comparison with a *TA* study on 5′-dGpdT-3′dinucleotide,[11] whose polarity, *i.e.* the order according to which two nucleobases are connected *via* the phosphodiester backbone, is opposite than that of **TG**.

The longest living transient species detected in 5′-dGpdT-3′ was attributed to the thymine triplet state (^{3}ππ*T).[11] However, the spectral shape of ^{3}ππ*T, studied by ns flash photolysis and peaking at 350 nm,[41] is very different than our *TAS* at 40 ps (Fig. 6a), exhibiting three well-defined absorption bands in the probed wavelength range (see Fig. S7a† for a comparison). These bands are absent from the 40 ps *TAS* determined for an equimolar mixture of dG and dT, shown on an appropriate scale in Fig. S8,† and from the ^{3}ππ*G(La) spectrum, peaking at 370 nm.[42] The 40 ps *TAS* (Fig. 6a) resembles instead the spectrum computed for the min-nπ*T state (Fig. 6b), which also exhibits three bands. The lifetime of the nπ* state in thymidine monophosphate is 130 ps,[43] explaining why it appears as a constant background in our measurements. We have not found any reference in the literature on the broad band *TA* spectra of nπ*T or nπ*G(La) states.

We assign the peak at 530 nm decaying with a time constant of 5.4 ps to a *CT* state. To obtain a rough evaluation of the *CT* state spectrum, we can consider an equimolar mixture of the guanosine radical cation and the thymidine radical anion, whose *TAS* have been obtained, respectively, by ns flash photolysis[44] and pulse radiolysis.[45] The resulting *TAS*, shown in Fig. S7b,† presents an absorption band around 505 nm. The overlap with that of the *CT* state of **TG** is not expected to be perfect for three reasons. (i) Not an entire atomic charge is transferred in the *CT* state (Table S5†), and as the amount of the transferred charge increases, the spectrum of the *CT* state shifts toward shorter wavelengths (Fig. S6b†). (ii) In a previous experimental and theoretical study, we reported that the spectral shape of the *CT* state in dinucleotides is affected by their polarity.[13] (iii) In pulse radiolysis experiments electrons give rise to additional transient species absorbing in the UV. The spectrum computed for the min-*CT* of *anti–syn* **TG** is shown in Fig. 6b, while the experimental *TAS* at 5 ps, when the contribution from localized ππ* states has practically vanished (Fig. 3a) in Fig. 6a; the comparison between the two spectra is improved after subtraction of the long-lived background *PA* at 40 ps. The 5 ps *TAS* spectrum exhibits an intense band at 380 nm and a second one in the visible, in good agreement with the computed min-*CT* spectrum (Fig. 6b).

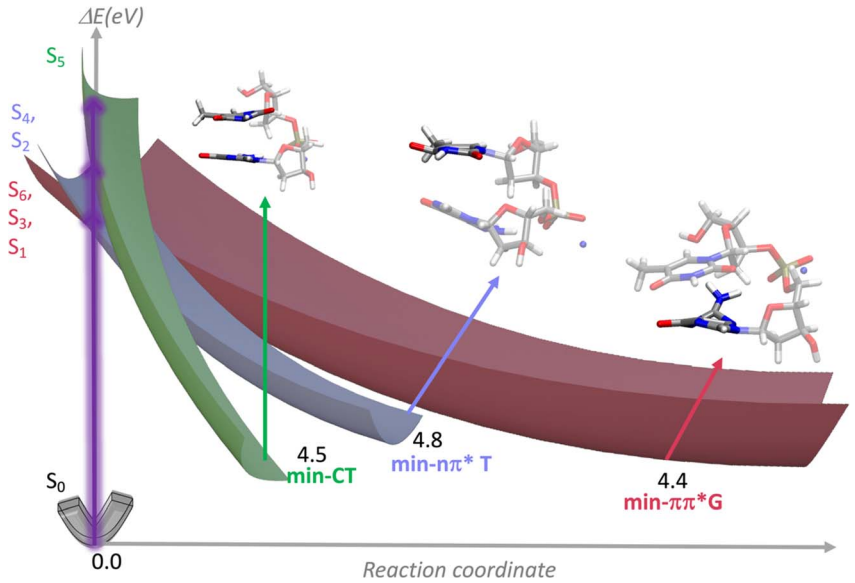

Fig. 5 Schematic representation of the *PES* associated with the 6 Franck–Condon states of *anti–syn* **TG** leading to three minima, whose structure and relative energy Δ*E* (eV) are also shown.

The measured lifetime of 5.44 ± 0.03 ps is about half of that reported for 5′-dGpdT-3′ (10–14 ps).[11,12] This is not surprising because the DNA polarity affects the excited state relaxation.[13] Thus, the lifetime of the *CT* state in 5′-dApdG-3′ (112 ps) was found to be shorter than that in 5′-dGpdA-3′ (170 ps).[13]

The build-up of a small *PA* band at ∼445 nm observed in Fig. 3b and its disappearance within 2–3 ps (Fig. 3c) are assigned, respectively, to T → G *ET* and to the decay of the ππ*G(La) state. Indeed, the dT *TAS* does not exhibit such a band (Fig. S4†), while it is present in the 50 fs *TAS* of dG. A previous theoretical study assigned this spectral feature to a minimum in the *PES* of the first excited state of dG.[46] Although a build-up at this wavelength is also observed for the free dG, it is significantly smaller compared to that found for **TG** (Fig. 7a). Moreover, the maximum intensity is reached within 60 fs for dG, as compared to 90 fs for **TG**. These build-up times correspond to relaxation processes and are not limited by the time resolution, as attested by Fig. S1.†

According to our calculations, population of the min-*CT*, whose *PA* bands are located at shorter wavelengths with respect to those of the initial Franck–Condon state S_5 (Fig. S6b†), is expected to induce a blue shift, in line with what is observed in Fig. 3b. The associated non-exponential dynamics (Fig. 4a), is explained by the fact that the process takes place within the restricted geometry defined by the *PES*. We remark that, in these spectral and temporal ranges, the *TAS* recorded for an equimolar mixture of mononucleotides do not exhibit any significant change either in the position or in the intensity of their maximum (Fig. S9†).

The slower blue shift of the low-energy band (Fig. 3c and 4b) is explained by the decay of the ππ*G(La) state. This is better illustrated by overlaying the position of λ_{max} between 0.2 and 2.5 ps with the dG decay averaged within the considered spectral range, 530–560 nm (Fig. 7b). It is further supported by the similar time constants derived by fits with mono-exponential functions of the spectral shift (0.61 ± 0.08 ps; Fig. 4b) and the dG decay (0.64 ± 0.03 ps). We stress that the latter value is not representative of the entire dG dynamics, which is very complex;[37–39,46,47] it simply reflects its behaviour within the

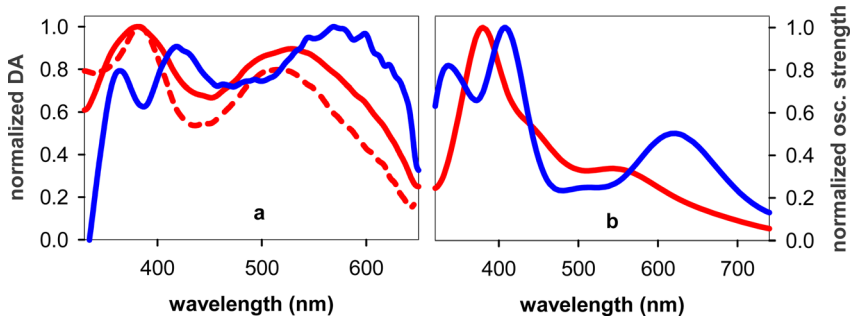

Fig. 6 Comparison between experimental *TAS* recorded for **TG** (a) with those computed for *anti–syn* **TG** (b); (a) *TAS* at 40 ps (blue) and 5 ps (red); the dashed red line corresponds to the difference between the *TAS* at 5 and 40 ps. (b) min-nπ*T (blue) and min-*CT* (red).

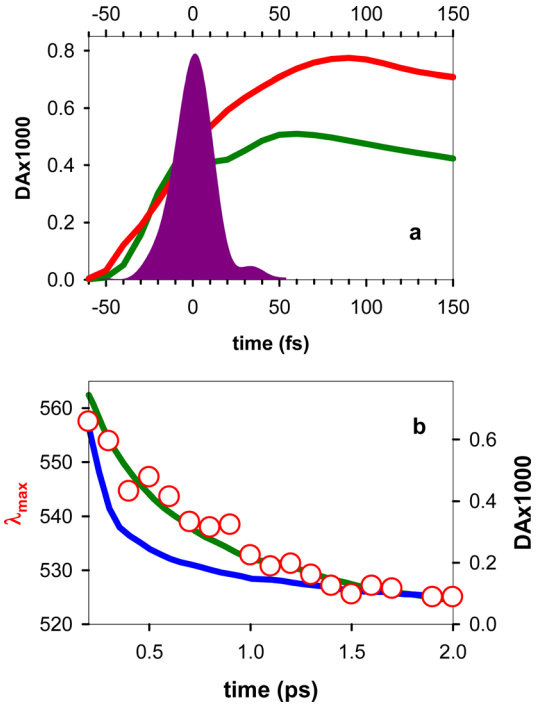

Fig. 7 (a) Rise of the *TA* signals at 445 nm recorded for **TG** (red) and a dG solution with equivalent concentration (green) at 445 nm; the temporal profile of the laser pulse is shown in violet. (b) Comparison of the dynamics observed for the shift of the low-energy band in the **TG** *TAS* (red circles) with the decays of dG (green) and dT (blue), averaged over the spectral range of the shift (530–560 nm).

spectral and temporal limits corresponding to Fig. 7b, where it is also clear that the dT decay follows a different pattern.

So far, we discussed the experimental *TAS* in the light of the relaxation pathways computed for *anti–syn* **TG**. Now we examine whether the other less stable conformers could be responsible for the three excited state *PES* minima that have been associated with the observed spectral evolution. The min-nπ*T is reached in all of them. The min-*CT* is encountered only for *syn–anti* **TG**. The pathway corresponding to T → G *ET* is detected for the *syn–syn* conformer.

Although *anti–syn* is the most stable **TG** conformer in the ground state and the fingerprints corresponding to the minima of its *PES* are detected in the experimental TAS, we cannot rule out that the other conformers are also present in solution, albeit with a much lower concentration. Similarly, it is quite possible that we have a contribution from unstacked nucleobases, mainly characterized by localized excited states; yet the lack of a negative signal due to the *SE* of $\pi\pi$*T, which does not correspond to a *PES* minimum in *anti–syn* **TG**, indicates that this contribution is rather low.

Global analysis

The multitude of the above discussed processes, associated with 3 minima in the 3 *PES* of each conformer and 2 for the unstacked nucleobases, giving rise to a complex network of excited states, is one reason why we have not based our analysis on global fits. The second and most important reason for avoiding analysis with exponential functions over the entire time domain explored in our experiments is related with the physics of the processes. As mentioned in the introduction, an excited state decays exponentially when its interactions with the environment are uniform within the three-dimensional space. In low-dimensional spaces the dynamics tend to be slower, described, for example, by stretched exponentials or exhibiting power-law patterns.[25,48] To correctly describe the dynamics in a given system, specific theoretical analysis and/or numerical simulations are required. We stress that the power-law function used to fit the spectral shift in Fig. 4a is a phenomenological approach, simply showing that the dynamics of the process is not exponential.

In any case, we did perform a global analysis within the framework of sequentially evolving species. Fig. S10† reports the evolution associated spectra (*EAS*) for an equimolar mixture of dT and dG. Five time constants (120 fs, 250 fs, 800 fs, 2.1 ps and 2 ns) are needed to fit the data, numerically close to those

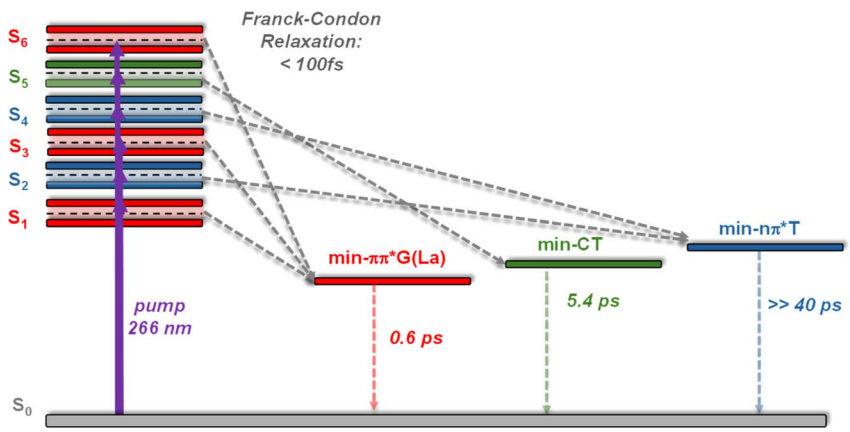

Fig. 8 Schematic drawing of the Franck–Condon excited states and the corresponding minima computed in the *PES* of *anti–syn* **TG**. In italics: dynamics determined from the *TAS* evolution. The relaxation time leading to min-nπ*T has not been observed, because the associated signal is too weak and blurred by those corresponding to other excited states; the 0.6 ps indicated for the decay of min-$\pi\pi$*G(La) corresponds only to the minimum absorbing in the red.[37–39,47]

reported by Kwok and co-workers for dT (150 fs and 760 fs)[40] and dG (200 fs, 790 fs and 2.0 ps)[38] using a lower temporal resolution. However, the similar time evolution of the individual nucleosides does not allow for their spectral discrimination within the studied equimolar mixture. As a result, instead of identifying distinct spectral signatures for each nucleoside, an average spectrum is obtained.

In the case of **TG**, the use of 4 exponential functions (50 fs, 380 fs, 4.5 ps and 2 ns) provides acceptable fits (see *EAS* in Fig. S11†). The spectral features corresponding to the time constants of 4.5 ps and 2 ns resemble those attributed to min-*CT* and min-nπ*T (Fig. S12†) but the evolution on shorter times, in particular, that corresponding to the complex decay of ππ*G(La), is not correctly resolved.

Conclusion

This article reports an important breakthrough in the study of photoinduced excited state relaxation in coupled nucleobases in solution. The novelties concern both the approach and the obtained results. Two main methodological innovations need to be underlined. On the one hand, this is the first observation of transient absorption spectra and dynamics on the sub-100-fs timescale. It was rendered possible by the exceptional combination of sensitivity and temporal resolution of our femtosecond *TA* setup. On the other hand, the interpretation of the results has been based on a battery of quantum chemistry calculations on the most stable geometry in the ground state, the Franck–Condon states, their evolution toward the excited state minima and the corresponding *TAS*. In this way, we circumvented the global fits with exponential functions, which are inadequate to describe evolution along potential energy surfaces.

Several compelling results emerged from our investigation.

(i) Our computations showed that the most stable conformation of **TG** involving stacked nucleobases (*anti–syn*) differs from that adopted by the T/G step in B-form duplexes (*anti–anti*), which has been implicitly considered for the interpretation of previous femtosecond measurements on dinucleotides.[11,13] The *anti–syn* conformation is encountered in G-Quadruplexes.[30]

(ii) The minima corresponding to relaxation pathways computed for the *anti–syn* **TG**, summarized in Fig. 8, are detected in the experimental *TAS*.

(iii) According to *TA* measurements, the *CT* state is reached within 100 fs, following non-exponential dynamics and decays with a lifetime of 5.4 ps. This the shortest lifetime ever determined for DNA dinucleotides,[8–14] and, probably, for any donor–acceptor pair of aromatic chromophores.

(iv) The *PES* leading to min-ππ*G(La) corresponds to T → G *ET*. The associated spectral evolution occurs within 90 fs. Such an ultrafast *ET* could be facilitated by a very small *CT* between the nucleobases characterizing the initial Franck–Condon state (Table 1). So far, ultrafast *ET* in DNA was considered to proceed exclusively *via* exciton states.[23]

(v) Several detailed studies, dealing with monomeric pyrimidines, reported population of nπ* states.[43,49,50] But so far, no experimental studies identified such states in dinucleotides or larger DNA multimeric systems composed of the major nucleobases.

The use of quantum chemistry calculations allowed a qualitative assignment of the dominant processes. In this way, we circumvented the global fits with exponential functions which, although they bring precious information on longer timescales, are inadequate to describe wave packet evolution along *PES* and/or systems involving a large number of transient species. Yet, the question of dynamical models that are appropriate to describe these processes remains open and requires specific work. We hope that our experimental results will inspire the future development of less time-consuming methods than those currently available that can be applied on large molecular systems.

Finally, an interesting perspective is to examine whether the ultrafast T → G energy transfer, detected in **TG**, also occurs in G-Quadruplexes. If this were the case, positioning peripheral thymines at the 5′ end with respect to the guanines of the G-core should further enhance their fluorescence. Such an enhancement is important because the intrinsic fluorescence of G-Quadruplexes is currently scrutinized in view of biosensors development.[3,51,52]

Methods

Transient absorption setup

Ultrafast *TA* experiments were conducted using a custom-built setup, employing an amplified Ti:Sapphire laser (Coherent Libra) that generates 100 fs pulses at a central wavelength of 800 nm, operating at a repetition rate of 1 kHz.[31,53] A fraction of the fundamental laser beam is first frequency-doubled and then directed to drive a broadband visible non-collinear optical parametric amplifier (NOPA). The output of the NOPA consists of broadband visible pulses, which are subsequently compressed using chirped dielectric mirrors. These compressed pulses are further frequency-doubled in a 20-μm-thick β-barium borate crystal, resulting in broadband UV pump pulses that can be tuned within the range of 250–300 nm. The generated UV pump pulses, fully characterized through two-dimensional spectral interferometry, are compressed to 24 fs (FWHM) duration with the help of a prism pair[54] (Fig. S13†). For the purpose of the experiment, the UV pump pulses are tuned to 266 nm. Broadband probe pulses, with spectrum spanning from 320 nm to 650 nm, were obtained by white-light continuum generation, focusing a portion of the laser fundamental beam onto a slowly moving 2-mm-thick CaF_2 plate. Pump and probe pulses are non-collinearly focused on the sample under study, with spot sizes of 180 μm and 95 μm, respectively. The relative pump and probe polarizations are adjusted to the magic angle (54.7°). The pump fluence is kept at 100 μJ cm^{-2}, resulting in differential absorption (DA) signals lower than 10^{-3}; in this way, the coherent artefact and solvated electrons stemming from two-photon ionization of the solvent are minimized. The transmitted probe spectrum is recorded by an optical multichannel analyser, operating at the full laser repetition rate. The temporal resolution is estimated to be sub-

30-fs. At 20 fs, although spectral intensities are not fully developed, spectral shapes in the visible are meaningful. During the experiment 6 mL of the solution kept flowing through a 1-mm-thick quartz cell controlled by a pump. For a detailed discussion of the temporal resolution in the UV *TA* experiments, see Section 1 in the ESI.†

Key experimental points

Dinucleotides are difficult to purify and residual mononucleotides may "contaminate" their proprieties. Therefore, purchased from Eurogentec, **TG** was purified by reverse phase HPLC and tested by MALDI-TOF (Fig. S14†). It was dissolved in phosphate buffer ($\sim$0.12 mol L^{-1}, pH 7.0). The concentration of absorbed photons (8×10^{-6} mol L^{-1}) was much lower than the dinucleotide concentration ($\sim 4 \times 10^{-3}$ mol L^{-1}), precluding two-photon absorption. Experiments on the monomeric chromophores were performed using the mononucleosides dT and dG in water, instead of the corresponding mononucleotides, which have a great propensity to aggregate in solutions containing salts.[55]

Computational details

We used quantum mechanical (QM) calculations, based on the Density Functional Theory (DFT) with the M052X functional,[56–58] the 6-31G(d) basis set. The solvent effect was taken into account *via* an implicit polarizable continuum model (PCM),[59] which was shown to reproduce experimental trends in a satisfactory way.[60,61] In our computations we included one Na^+ ion per dinucleotide so as to keep the system electrically neutral.

The vertical absorption energies of the different excited states and the corresponding *PES* were characterized using the above-described methodologies, but resorting to the time-dependent version (TD-DFT). The charge transfer character was computed by a simple Mulliken population analysis in terms of δq, *i.e.*, the difference between the charges in the excited state and in the ground state.

For the *TA* spectra, the transition dipole moments between the excited states were obtained by a multifunctional analyser (multiwfn program).[62] For comparison with the experimental spectra, the computed ones were shifted by −0.65 eV. Such a shift, typical for this level of calculation, matches the difference between the energy computed for the lowest bright state (La) of dG in water and the corresponding value derived from deconvolution of the experimental spectrum (Fig. 2 in ref. 63). Subsequently, we applied a phenomenological broadening *via* a Gaussian function with half width at half maximum of 0.2 eV.

Data availability

The data that support the findings of this study are available in the ESI† and the on: **https://doi.org/10.5281/zenodo.11453876**. They are also available upon request from the corresponding authors.

Author contributions

Conceptualization: LMF, GC, DM; data curation: VP, LMF; formal analysis: VP, LMF, EB, DM; funding acquisition: GC, MM, DM; investigation: VP, LMF, LU; methodology: LMF, GC, MM; supervision: GC, MM; validation: all authors; visualization: VP, LMF, EB, DM; writing original draft: VP, LMF, DM; writing – review & editing: VP, LMF, GC, EB, DM.

Conflicts of interest

There are no conflicts to declare.

Acknowledgements

This work has received funding from the European Union's Horizon 2020 research and innovation programme under the Marie Sklodowska-Curie ITN programme (grant No. 765266 – LightDyNAmics and grant No. 812992 – MUSIQ). G.C. acknowledges financial support by the European Union's NextGenerationEU Programme with the I-PHOQS Infrastructure [IR0000016, ID D2B8D520, CUP B53C22001750006] "Integrated infrastructure initiative in Photonic and Quantum Sciences". L. M.-F. is indebted to the Galician Supercomputing Center for the access granted to its supercomputing infrastructure.

References

1 *DNA Photodamage: From Light Absorption to Cellular Responses and Skin Cancer*, ed. R. Improta and T. Douki, RSC, Cambridge, 2021.
2 M. E. Barbinta-Patrascu and S. M. Iordache, DNA - the fascinating biomacromolecule in optoelectronics and photonics applications, *J. Optoelectron. Adv. Mater.*, 2022, **24**, 563–575.
3 D. Markovitsi, Processes triggered in guanine quadruplexes by direct absorption of UV radiation: From fundamental studies toward optoelectronic biosensors, *Photochem. Photobiol.*, 2024, **100**, 262–274.
4 J. Cadet and T. Douki, Formation of UV-induced DNA damage contributing to skin cancer development, *Photochem. Photobiol. Sci.*, 2018, **17**, 1816–1841.
5 E. Balanikas, A. Banyasz, T. Douki, G. Baldacchino and D. Markovitsi, Guanine Radicals Induced in DNA by Low-Energy Photoionization, *Acc. Chem. Res.*, 2020, **53**, 1511–1519.
6 L. Martinez Fernandez and R. Improrta, in *DNA Photodamage: From Light Absorption to Cellular Responses and Skin Cancer*, ed. R. Improta and T. Douki, RSC, Cambridge, 2021, doi: DOI: **10.1039/9781839165580**, ch. 2, pp. 17–36.
7 H. A. Wagenknecht, Remote Photodamaging of DNA by Photoinduced Energy Transport, *Chembiochem*, 2022, **23**, e202100265.
8 I. Buchvarov, Q. Wang, M. Raytchev, A. Trifonov and T. Fiebig, Electronic energy delocalization and dissipation

in single- and double-stranded DNA, *Proc. Natl. Acad. Sci. U.S.A.*, 2007, **104**, 4794–4797.
9 M. C. Stuhldreier and F. Temps, Ultrafast photo-initiated molecular quantum dynamics in the DNA dinucleotide d(ApG) revealed by broadband transient absorption spectroscopy, *Faraday Discuss*, 2013, **163**, 173–188.
10 J. Chen and B. Kohler, Base Stacking in Adenosine Dimers Revealed by Femtosecond Transient Absorption Spectroscopy, *J. Am. Chem. Soc.*, 2014, **136**, 6362–6372.
11 M. Duchi, M. P. O'Hagan, R. Kumar, S. J. Bennie, M. C. Galan, B. F. E. Curchod and T. A. A. Oliver, Exploring ultraviolet photoinduced charge-transfer dynamics in a model dinucleotide of guanine and thymine, *Phys. Chem. Chem. Phys.*, 2019, **21**, 14407–14417.
12 C. L. Kufner, W. Zinth and D. B. Bucher, UV-Induced Charge-Transfer States in Short Guanosine-Containing DNA Oligonucleotides, *Chembiochem*, 2020, **21**, 2306–2310.
13 V. Petropoulos, L. Uboldi, M. Maiuri, G. Cerullo, L. Martinez-Fernandez, E. Balanikas and D. Markovitsi, Effect of the DNA polarity on the relaxation of its electronic excited states, *J. Phys. Chem. Lett.*, 2023, **14**, 10219–10224.
14 T. Takaya, C. Su, K. de La Harpe, C. E. Crespo-Hernandez and B. Kohler, UV excitation of single DNA and RNA strands produces high yields of exciplex states between two stacked bases, *Proc. Natl. Acad. Sci. U. S. A.*, 2008, **105**, 10285–10290.
15 J. Chen, Y. Zhang and B. Kohler, Excited states in DNA strands investigated by ultrafast laser spectroscopy, *Top. Curr. Chem.*, 2015, **356**, 39–87.
16 W. J. Schreier, P. Gilch and W. Zinth, Early Events of DNA Photodamage, *Annu. Rev. Phys. Chem.*, 2015, **66**, 497–519.
17 W. M. Kwok, C. S. Ma and D. L. Phillips, "Bright" and "Dark" excited states of an alternating AT oligomer characterized by femtosecond broadband spectroscopy, *J. Phys. Chem. B*, 2009, **113**, 11527–11534.
18 C. S. Ma, R. C.-T. Chan, C. T.-L. Chan, A. K.-W. Wong and W.-M. Kwok, Real-time Monitoring Excitation Dynamics of Human Telomeric Guanine Quadruplexes: Effect of Folding Topology, Metal Cation, and Confinement by Nanocavity Water Pool, *J. Phys. Chem. Lett.*, 2019, **10**, 7577–7585.
19 G. W. Doorley, D. A. McGovern, M. W. George, M. Towrie, A. W. Parker, J. M. Kelly and S. J. Quinn, Picosecond transient infrared study of the ultrafast deactivation processes of electronically excited B-DNA and Z-DNA forms of $[poly(dG\text{-}dC)]_2$, *Angew. Chem., Int. Ed.*, 2009, **48**, 123–127.
20 G. W. Doorley, M. Wojdyla, G. W. Watson, M. Towrie, A. W. Parker, J. M. Kelly and S. J. Quinn, Tracking DNA Excited States by Picosecond-Time-Resolved Infrared Spectroscopy: Signature Band for a Charge-Transfer Excited State in Stacked Adenine-Thymine Systems, *J. Phys. Chem. Lett.*, 2013, **4**, 2739–2744.
21 P. M. Keane, M. Wojdyla, G. W. Doorley, J. M. Kelly, A. W. Parker, I. P. Clark, G. M. Greetham, M. Towrie, L. M. Magno and S. J. Quinn, Long-lived excited states in i-motif DNA studied by picosecond time-resolved IR spectroscopy, *Chem. Commun.*, 2014, **50**, 2990–2992.
22 L. Martínez-Fernández, J. A. Green, L. Esposito, M. Y. Jouybari, Y. Y. Zhang, F. Santoro, B. Kohler and R. Improta, The photoactivated dynamics of dGpdC and dCpdG sequences in DNA: a comprehensive quantum mechanical study, *Chem. Sci.*, 2024, 9676–9693.
23 T. Gustavsson and D. Markovitsi, Fundamentals of the Intrinsic DNA Fluorescence, *Acc. Chem. Res.*, 2021, **54**, 1226–1235.
24 A. Blumen, J. Klafter and G. Zumofen, in *Optical spectroscopy of glasses*, ed. I. Zschokke, Springer, Dordecht, the Netherlands, 1986, pp. 199–265.
25 J. M. Drake, J. Klafter and P. Levitz, Chemical and Biological Microstructures as Probed by Dynamical Processes, *Science*, 1991, **251**, 1574–1579.
26 D. Markovitsi, A. Germain, P. Millie, I. Lécuyer, L. Gallos, P. Argyrakis, H. Bengs and H. Ringsdorf, Triphenylene columnar liquid crystals: excited states and energy transfer, *J. Phys. Chem.*, 1995, **99**, 1005–1017.
27 K. Y. Guslienko, Magnetic vortex state stability, reversal and dynamics in restricted geometries, *J. Nanosci. Nanotechnol.*, 2008, **8**, 2745–2760.
28 O. Benichou, C. Chevalier, J. Klafter, B. Meyer and R. Voituriez, Geometry-controlled kinetics, *Nat. Chem.*, 2010, **2**, 472–477.
29 M. Zarea, R. Carmieli, M. A. Ratner and M. R. Wasielewski, Spin Dynamics of Radical Pairs with Restricted Geometries and Strong Exchange Coupling: The Role of Hyperfine Coupling, *J. Phys. Chem. A*, 2014, **118**, 4249–4255.
30 J. L. Chen, M. P. Cheng, G. F. Salgado, P. Stadlbauer, X. B. Zhang, S. Amrane, A. Guédin, F. N. He, J. Sponer, H. X. Ju, J. L. Mergny and J. Zhou, The beginning and the end: flanking nucleotides induce a parallel G-quadruplex topology, *Nucleic Acids Res.*, 2021, **49**, 9548–9559.
31 R. Borrego-Varillas, L. Ganzer, G. Cerullo and C. Manzoni, Ultraviolet Transient Absorption Spectrometer with Sub-20-fs Time Resolution, *Appl. Sci.*, 2018, **8**, 989.
32 D. Onidas, D. Markovitsi, S. Marguet, A. Sharonov and T. Gustavsson, Fluorescence properties of DNA nucleosides and nucleotides: a refined steady-state and femtosecond investigation, *J. Phys. Chem. B*, 2002, **106**, 11367–11374.
33 D. Varsano, R. Di Felice, M. A. L. Marques and A. Rubio, A TDDFT study of the excited states of DNA bases and their assemblies, *J. Phys. Chem. B*, 2006, **110**, 7129–7138.
34 F. Plasser, A. Aquino, H. Lischka and D. Nachtigallová, Electronic Excitation Processes in Single-Strand and Double-Strand DNA: A Computational Approach, *Top. Curr. Chem.*, 2015, **356**, 1–38.
35 E. Balanikas, L. Martinez-Fernadez, R. Improta, P. Podbevsek, G. Baldacchino and D. Markovitsi, The Structural Duality of Nucleobases in Guanine Quadruplexes Controls Their Low-Energy Photoionization, *J. Phys. Chem. Lett.*, 2021, **12**, 8309–8313.
36 E. Palecek and M. Bartosik, Electrochemistry of Nucleic Acids, *Chem. Rev.*, 2012, **112**, 3427–3481.
37 V. Karunakaran, K. Kleinermanns, R. Improta and S. A. Kovalenko, Photoinduced dynamics of guanosine monophosphate in water from broad-band transient

absorption spectroscopy and quantum-chemical calculations, *J. Am. Chem. Soc.*, 2009, **131**, 5839–5850.

38 C. C.-W. Cheng, C. Ma, C. T.-L. Chan, K. Y.-F. Ho and W.-M. Kwok, The solvent effect and identification of a weakly emissive state in nonradiative dynamics of guanine nucleosides and nucleotides - a combined femtosecond broadband time-resolved fluorescence and transient absorption study, *Photochem. Photobiol. Sci.*, 2013, **12**, 1351–1365.

39 S. E. Krul, S. J. Hoehn, K. J. Feierabend and C. E. Crespo-Hernández, Excited state dynamics of 7-deazaguanosine and guanosine 5′-monophosphate, *J. Chem. Phys.*, 2021, **154**, 075103.

40 W. M. Kwok, C. Ma and D. L. Phillips, A doorway state leads to photostability or triplet photodamage in thymine DNA, *J. Am. Chem. Soc.*, 2008, **130**, 5131–5139.

41 S. Marguet and D. Markovitsi, Time-resolved study of thymine dimer formation, *J. Am. Chem. Soc.*, 2005, **127**, 5780–5781.

42 P. D. Wood and R. Redmond, Triplet state interactions between nucleic acid bases in solution at room temperature: intermolecular energy and electron transfer, *J. Am. Chem. Soc.*, 1996, **118**, 4256–4263.

43 P. M. Hare, C. Crespo-Hernández and B. Kohler, Internal conversion to electronic ground state occurs *via* two distinct pathways for pyrimidine bases in aqueous solution, *Proc. Natl. Acad. Sci. U. S. A.*, 2007, **104**, 435–440.

44 L. P. Candeias and S. Steenken, Ionization of purine nucleosides and nucleotides and their components by 193-nm laser photolysis in aqueous solution: model studies for oxidative damage of DNA, *J. Am. Chem. Soc.*, 1992, **114**, 699–704.

45 R. Yamagami, K. Kobayashi and S. Tagawa, Formation of Spectral Intermediate G-C and A-T Anion Complex in Duplex DNA Studied by Pulse Radiolysis, *J. Am. Chem. Soc.*, 2008, **130**, 14772–14777.

46 J. Ortín-Fernández, J. González-Vázquez, L. Martínez-Fernández and I. Corral, Molecular Identification of the Transient Species Mediating the Deactivation Dynamics of Solvated Guanosine and Deazaguanosine, *Molecules*, 2022, **27**, 989.

47 Y. Zhang, R. Improta and B. Kohler, Mode-specific vibrational relaxation of photoexcited guanosine 5'-monophosphate and its acid form: a femtosecond broadband mid-IR transient absorption and theoretical study, *Phys. Chem. Chem. Phys.*, 2014, **16**, 1487–1499.

48 M. F. Shlessinger and A. W. Montroll, On the Willams-Watts function of dielectric relaxation, *Proc. Natl. Acad. Sci. U. S. A.*, 1984, **81**, 1280–1283.

49 Y. Miura, Y. Yamamoto, S. Karashima, N. Orimo, A. Hara, K. Fukuoka, T. Ishiyama and T. Suzuki, Formation of Long-Lived Dark States during Electronic Relaxation of Pyrimidine Nucleobases Studied Using Extreme Ultraviolet Time-Resolved Photoelectron Spectroscopy, *J. Am. Chem. Soc.*, 2023, **145**, 3369–3381.

50 S. J. Hoehn, S. E. Krul, M. M. Pogharian, E. Mao and C. E. Crespo-Hernández, Photochemical Stability of 5-Methylcytidine Relative to Cytidine: Photophysical Insight for mRNA Therapeutic Applications, *J. Phys. Chem. Lett.*, 2023, **14**, 10856–10862.

51 C. Lu, A. Lopez, J. K. Zheng and J. W. Liu, Using the Intrinsic Fluorescence of DNA to Characterize Aptamer Binding, *Molecules*, 2022, **27**, 7809.

52 A. Lopez and J. Liu, Probing metal-dependent G-quadruplexes using the intrinsic fluorescence of DNA, *Chem. Commun.*, 2022, **58**, 10225–10228.

53 D. Polli, L. Luer and G. Cerullo, High-time-resolution pump-probe system with broadband detection for the study of time-domain vibrational dynamics, *Rev. Sci. Instrum.*, 2007, **78**, 103108.

54 R. Borrego-Varillas, A. Oriana, F. Branchi, S. De Silvestri, G. Cerullo and C. Manzoni, Optimized ancillae generation for ultra-broadband two-dimensional spectral-shearing interferometry, *J. Opt. Soc. Am. B*, 2015, **32**, 1851–1855.

55 E. Baldassarri, M. G. Ortore, F. Spinozzi, A. Round, C. Ferrero and P. Mariani, K^+ *vs.* Na^+ Effects on the Self-Assembly of Guanosine 5′-Monophosphate: A Solution SAXS Structural Study, *Nanomaterials*, 2020, **10**, 629.

56 Y. Zhao, N. E. Schultz and D. G. Truhlar, Design of density functionals by combining the method of constraint satisfaction with parametrization for thermochemistry, thermochemical kinetics, and noncovalent interactions, *J. Chem. Theory Comput.*, 2006, **2**, 364–382.

57 Y. Zhao and D. G. Truhlar, Density functionals with broad applicability in chemistry, *Acc. Chem. Res.*, 2008, **41**, 157–167.

58 R. Improta, F. Santoro and L. Blancafort, Quantum Mechanical Studies on the Photophysics and the Photochemistry of Nucleic Acids and Nucleobases, *Chem. Rev.*, 2016, **116**, 3540–3593.

59 J. Tomasi, B. Mennucci and R. Cammi, Quantum mechanical continuum solvation models, *Chem. Rev.*, 2005, **105**, 2999–3093.

60 L. Martinez-Fernandez, A. J. Pepino, J. Segarra-Marti, A. Banyasz, M. Garavelli and R. Improta, Computing the Absorption and Emission Spectra of 5-Methylcytidine in Different Solvents: A Test-Case for Different Solvation Models, *J. Chem. Theor. Comput.*, 2016, **12**, 4430–4439.

61 L. Martinez-Fernandez, F. Santoro and R. Improta, Nucleic Acids as a Playground for the Computational Study of the Photophysics and Photochemistry of Multichromophore Assemblies, *Acc. Chem. Res.*, 2022, **55**, 2077–2087.

62 T. Lu and F. W. Chen, Multiwfn: A multifunctional wavefunction analyzer, *J. Comput. Chem.*, 2012, **33**, 580–592.

63 B. Bouvier, T. Gustavsson, D. Markovitsi and P. Millié, Dipolar coupling between electronic transitions of the DNA bases and its relevance to exciton states in double helices, *Chem. Phys.*, 2002, **275**, 75–92.